Published in: Journal of the European Ceramic Society (2011), vol. 31, pp. 1075-1086.
Status: Postprint (Author's version)

$YBa_2Cu_3O_{7-x}$ dispersion in iodine acetone for Electrophoretic Deposition: Surface charging mechanism in a halogenated organic media

Laurent Dusoulier[a,b], Rudi Cloots[a], Bénédicte Vertruyen[a], Rodrigo Moreno[c], O. Burgos-Montes[c,d], Begoña Ferrari*[c]

[a] Bât B6 Chimie Inorganique Structurale, Université de Liège, allée de la Chimie 3, 4000, Liège 1, Belgique. Tel: +32 4 3663436, Fax: +32 4 3663413. l.dusoulier@gmail.com; rcloots@ulg.ac.be; B.Vertruyen@ulg.ac.be.

[b] Royal Military Academy, CISS department, Brussels, Belgium.

[c] Instituto de Cerámica y Vidrio, CSIC, Campus de Cantoblanco, c/Kelsen 5, 28049, Madrid, Spain. Tel: +34 91 7355840, Fax: +34 91 7355843.
rmoreno@icv.csic.es; oburgos@icv.csic.es; bferrari@icv.csic.es.

[d] Instituto de Ciencias de la Construcción Eduardo Torroja, CSIC, c/Serrano Galvache 4, 28033, Madrid, Spain. Tel: +34 91 3020440, Fax: +34 91 3020700.
oburgos@ietcc.csic.es

Abstract

Electrophoretic Deposition (EPD) performance strongly depends on the particles surface chemistry and the ability to manipulate surface-liquid interfaces. In this study an extensive investigation of YBCO suspension in dry acetone, acetone-water mixtures and acetone-iodine is reported. Chemical instability of YBCO particles determines their colloidal behaviour. Charging mechanism of particles has therefore had to be deeply investigated for complete dispersion understanding. In order to determine the conditions of the YBCO suspension stability, measurements of pH, conductivity, zeta-potential, settling tests, modelling of the particle networks and electrophoretic deposition were done. The influence of the water and iodine concentration, and their role as stabilizers was evaluated. Based on experimental results, pair particle potentials were calculated and then different charging mechanisms of YBCO surfaces in acetone were proposed.

Keywords

Suspensions, Shaping, Films, Oxide Superconductors, Acetone Halogenation

1. Introduction

Electrophoretic deposition (EPD) technique is a suitable method to produce a wide range of structures and materials [1, 2]. This coating process is based on the migration of charged particles in a colloidal suspension by the application of an electric field between two electrodes. Once at the electrode, particles coagulate and solvent evaporates. During EPD, electric field is the driven force promoting particle packing, so film density depends on the solvent evaporation but also on the electric field strength. Consequently, particles surface chemistry and properties of surface-liquid interfaces strongly affects to the homogeneity and reliability of films shaped by EPD

$YBa_2Cu_3O_{7-x}$ (YBCO) is the current material of choice for second-generation superconducting wires. High-Tc superconductor research has been dealing with the properties of the final material, but today it is focus on the improvement of YBCO coated conductor fabrication [3-5]. In this sense EPD should be considered as a potential applicable technique, offering a real possibility of industrial scalability and reliability. In fact, EPD has been successfully considered for applications such as magnetic shielding in low frequencies [6-12]. However, much effort is still necessary to understand and control the complex colloidal behaviour and the surface reactions occurring when YBCO powders are dispersed in a liquid. Degradation of YBCO in water has been observed, mainly due to an incongruent dissolution of Ba^{2+}. Later carbonation and/or hydroxylation of Ba^{2+} [13, 14] determine the surface charge behaviour of YBCO in aqueous suspensions [15-18].

Organic solvents have been therefore used for EPD of YBCO, i.e. acetone [10, 12, 19-32], isobutylmethylketone [11], propanol and butanol [31, 32], acetone being the most used solvent. In acetone, a negative value of zeta potential for 0.01 g/l YBCO suspensions have been determined by Koura et al. [20], while more concentrated suspensions promote a positive surface charge, leading to cathodic deposition [12, 21-35, 31, 32]. Other studies show that it is customary to use iodine (I_2) as stabiliser in acetone [10, 12, 19, 20, 27-30]. Zeta-potentials of YBCO in acetone-I_2 solutions are always positive, forming also cathodic deposits.

Positive surfaces have been measured for other materials dispersed in I_2 solutions in acetone, i.e. SiO_2 [19, 33], V_2O_5 [34], Wollastonite [35], Zirconia stabilised with Yttria (YSZ) [36, 37], B [38], TiO_2 [39-41], LSCF, CGO [42] and LSGM [43, 44]. Moreover, I_2 has been also used as dispersing agent in other organic solvents, such as acetilacetone (AcAc) [45-48], isopropanol (IPA) [49-51] or a mixture of acetone (Ac) or acetilacetone and ethanol (EtOH) [37, 42, 52-55].

Charging mechanisms of oxide particles in I_2 solutions in acetone have been proposed in the literature. The mechanism widely used considers the formation of iodoacetone in the presence of H_2O (equation 1), suggesting that particle surfaces become positive as a consequence of the proton formation during the acetone iodination [19, 20, 56]. A similar mechanism was proposed in other organic solvents [45, 49-53].

$$(CH_3)_2CO + I_2 \leftrightarrow CH_3C(OH)CH_2 \rightarrow CH_3COCH_2I + I^- + H^+ \quad (1)$$

Table 1 summarises the main results for EPD studies using I_2 as dispersing agent. Collected data are related to the characterization of particles and suspensions, attending to optimal conditions to obtain deposits by EPD. Most of them are devoted to YSZ and YBCO particles with different size and surface area. The main suspension parameters measured are pH, conductivity and zeta potential. In most of these studies concentrated suspensions (10 g/l) have been prepared to shape films by EPD.

Results summarised in table 1 show that liquid medium acidulates with I_2 concentration (from 0 to 1 g/l). Acidification of organic medium by I_2 addition was expected due to the I_2 acidic character [57]. Lee et al. [50] and Chen et al. [52] measured a decrease of the operational pH (7-2) with the I_2 addition (until 1 g/l) in YSZ suspensions prepared in isopropanol and acetone-ethanol, respectively. However, Koura et al. [20] measured a slight variation of the proton concentration in acetone when adding I_2 until 8 g/l in YBCO suspensions. Moreover, suspensions conductivities measured were extremely different in ketones and alcoholic media for similar solid loadings, corresponding to differences among solvent dielectric constants [58]. Conductivities of YSZ suspension in alcohols range from 1 to 12-14 mS/cm as a function of I_2 addition (0-1 g/l), while maintain below 0.2 mS/cm for reported YBCO suspensions in acetone.

Otherwise, zeta potential of YSZ/isopropanol and YBCO/acetone behaves similarly with I_2 addition. In all cases, zeta potential sharply increases resulting in positively charged particles with a small addition of I_2. Generally, a maximum zeta potential was achieved at I_2 concentrations ranging 0.2-0.6 g/l, being independent of larger additions. Suddenly, a maximum of zeta potential results in the obtention of heavier and homogeneous films by EPD. Higher zeta potential values were measured in ketones, but optimal amount of I_2 depends on the particle characteristics (size and specific surface area) [50, 52].

The aim of this work is to analyse in depth the mechanism of surface charging of YBCO in acetone, and key parameters to control the suspension stability and the subsequent processing. Two main sections are developed in view to understand the charging mechanism. Firstly the influence of water in acetone suspensions has been determined. Later, the effect of iodine as stabilizer in acetone has been analysed. Based on the results, a new approach to explain the role of water and I_2 in the charging mechanism of YBCO powders in acetone has been proposed.

2. Materials and Methods

As starting material a commercial $YBa_2Cu_3O_{7-x}$ (99.9% purity) powder from Alfa-Aesar (Germany) was used. A particle size around 4 µm, a specific surface of 1.4 m^2/g and a density of 5.91 g/cm^3 are the main characteristic of this powder. Particle size distribution was determined by laser diffraction particle size analysis (Mastersizer S, Malvern, UK), surface area by single point N_2 adsorption (BET Monosorb, Quantachrome, USA), and density by He-multipicnometry (Quantachrome, USA). No pre-treatments were made on the powder for suspension preparation. Two grades of acetone were used: technical grade (estimated H_2O content of 2.5 vol.%) and grade HPLC (H_2O< 0.01 vol.%). Deionised H_2O and I_2 (ref. A12278, Alfa-Aesar, Germany) were added to dry acetone as stabilizers.

Acetone solutions of I_2 up to 1 g/l were considered as suspension medium. UV-Visible adsorption (Perkin-Elmer, UV-Vis. spectrometer, Lambda 14P, UK) measurements were done to follow I_2 dissolution in acetone. A standard glass electrode was used to measure pH and conductivity (0.1 cm^{-1} conductimetry electrode). Although the operational pH concept should be used to study acid-base reactions in non-aqueous systems [59], in this work, pH was measured using a pH-meter calibrated for aqueous media to allow comparison of our own results. The "operational pH" measured using a pH meter calibrated for aqueous solvents differs from the real pa_H in a non-aqueous solvent (equation 2 at 25°C):

$$pH = pa_H + \frac{\Delta E_j}{0.05916} \quad (2)$$

where pa_H (=-log a_H) is the negative logarithm of the proton activity in a non-aqueous solvent, ΔE_j is the residual junction potential encountered in the standardization and testing step of a standard pH meter.

Suspensions were dispersed applying ultrasonication (Hielscher UP400S probe, Germany) during 30 sec in a glass container. Suspensions were maintained stirring at room conditions and pH was measured during 40 min after sonication. To study the surface behaviour of YBCO powders, suspensions were prepared: i) in technical grade acetone, where different solid contents were considered ranging from 0.1-10 g/l, ii) in dry acetone, where different amounts of water was added to 0.1 g/l YBCO suspension, and iii) in 10 g/l YBCO suspensions in technical acetone considering I_2 concentrations up to 0.5 g/l.

Stability studies were performed in terms of pH, conductivity, zeta potential and settling measurements. Zeta potential was done by laser Doppler velocimetry (Zetasizer NanoZS, Malvern, UK). Values were calculated from mobility data considering the Smoluchowski approximation for relative large particles and short Debye lengths.

Finally, YBCO coatings were shaped by EPD on nickel foils (Goodfellow, 99%) of 40 x 15 x 0.5 mm. EPD suspensions were prepared in different mixtures of dry acetone and water, and solutions of I_2 in technical grade acetone. The counter electrode was also a nickel foil of similar dimensions, separated from the work electrode by a distance of 2 cm in the electrophoresis cell. EPD was done under potentiostatic conditions using a high voltage power source (DC Apelex PS9009TX, France). The voltage applied in all cases was 200V during times up to 180 seconds. Samples were dried at room conditions after EPD, and the mass of each deposit was characterized by gravimetry.

3. Results and discussion

3.1. Dispersions in water-acetone mixtures for EPD.

It has been demonstrated elsewhere [18] that surface dissolution occurs when YBCO particles are suspended in water. Carbonation and Hydroxilation of solved ions affects to the concentration of potential determining ions (H^+ and OH^+), fixing the suspension stability. It is well known that those reactions may also occur in technical grade acetone at room conditions. Therefore, the surface behaviour of YBCO in acetone have to be also evaluated in terms of pH, conductivity and zeta potential, taking as variables the concentration of solids and water at the suspensions.

In this study, suspensions were prepared using technical acetone (water content of 2.5 vol.%) at YBCO concentrations of 0.1, 1 and 10 g/l. The pH evolution was measured during this time, and plotted in figure 1. The pH of 0.1 and 1 g/l suspensions varies from 9.4 to 8.9, and from 9.3 to 9.0 in 40 min, respectively, while the pH of the 10 g/l suspension changes from 9.5 to 8.6 in 20 min. An acidification tendency of the suspension media can be noted when solid concentration increases. Although suspensions are prepared in acetone both, the environmental humidity and the water content of technical grade acetone, promotes the slow carbonation of the Ba^{2+} leached from the YBCO particle surfaces [18]. The surrounding conditions of YBCO particles are a consequence of the powder dissolution and related reactions. Hence, low chemical stability of YBCO surfaces is also expected to determine dispersing conditions in acetone.

Figure 2 shows the variation of zeta potential with the amount of water added to 0.1 g/l suspensions prepared in dry acetone (curve a), and with YBCO concentration at suspensions prepared in technical grade acetone, (curve b).

In curve a, to avoid as much as possible YBCO dissolution, 0.1 g/l suspensions in dry acetone were considered. Then, different amounts of water (up to 12 vol.%) have been added to study their effect in the suspension stability. YBCO particles in dry acetone develop a strongly negative surface charge (-35 mV) as shown at curve a in figure 2. Strong negative surfaces (> 30 mV) maintain until water content of 3 vol.%. Zeta potential absolute values decrease with higher water additions, achieving zero at 7 vol.%. YBCO particles maintain zero zeta potential, or even reverse their surface charge for water contents around 12 vol.%. In all cases, suspension conductivity maintains below the technical accuracy of the conductimeter (0.2 µS/cm).

Similarly in curve b, zeta potential strongly changes with solid content in suspensions prepared in technical grade acetone. In fact, negative surfaces (-38 mV) in 0.1 g/l suspensions become positive at solid concentrations over 1.5 g/l. Nevertheless, a strong positive zeta potential (+30 mV) was measured for 10 g/l suspensions, whereas conductivity maintains always constant and below 0.2 µS/cm.

It is important to note that comparable zeta potential values have been measured for similar suspensions prepared under different conditions. In curve a, zeta potential of 0.1 g/l suspension prepared through the addition of 3 vol.% of deionised water to dry acetone is marked, while the value emphasised in curve b is the measure of 0.1 g/l suspension directly prepared in technical grade acetone (2.5 vol.% water content). Subsequently, results plotted in figure 1 and 2 (curve b) indicate the charge reversal is a consequence of the medium acidification promoted by the solid increase in presence of water. Otherwise, the development of charged surfaces in 10 g/l suspensions (+30 mV) has not any effect in the conductivity.

Consequently, YBCO surface reactions affect to the surface charge even in organic media [18]. Indeed, both suspension parameters solids and water content determine YBCO particle stability in acetone, being key for later shaping process.

Table 2 summarises the sense and deposition of the particle electrophoresis for different suspensions. Diluted suspension (0.1 g/l) of YBCO in dry acetone represents in this work the most favourable conditions to avoid YBCO dissolution. The surface of the YBCO particles in dry acetone is negative, as plotted in figure 2 (curve b), and deposition takes place at the anode during EPD. However, reliability of EPD with 0.1 g/l suspensions in technical grade acetone is very low. Deposition mainly occurs at the anode (table 2), as expected for negative zeta potentials in figure 2, but occasionally deposition takes also place on both electrodes, simultaneously. Kinetics of Ba^{2+} carbonation at room conditions in the presence of a small amount of water (2.5 vol.%) affects to the particle charging mechanism, especially for low solid contents. Particle surface should become positive after the homogenization time as a consequence of the medium acidification, YBCO depositing in the cathode.

Cathodic deposition occurs for 1 and 10 g/l suspensions. This was expected for 10 g/l suspensions in technical grade acetone, due to the strongly positive character of particle surfaces, and also for 1 g/l suspension attending to the low accuracy of zeta potential measurements in figure 2, curve b. However, it was unexpected for suspensions prepared in dry acetone. Since EPD tests were performed at room conditions, cathodic deposition for dry acetone evidences the effect of the hygroscopic character of the solvent, affecting the YBCO surface stability, stepping up by a higher amount of powder in suspension.

Figure 3 plots the variation of the suspension conductivity and the deposited mass as a function of water content at the solvent, for EPD in 10 g/l suspensions at 200 V for 180 s. Pictures within this figure show the appearance of the obtained deposits for water contents of 2.9 (b), 6.5 (c) and 10.7 vol.% (d). As expected the suspension conductivity increases with the amount of water, from values below 0.5 µS/cm for technical grade acetone to 6 µS/cm. Regarding the deposit quality, When dry acetone was used as dispersing media, the YBCO particles deposited heterogeneously in the anode. The addition of a small amount of water leads to a poor and heterogeneous deposition as figure 3b shows. The increments in water contents to a range between 6.5 to 8 vol.%, leads to uniform YBCO coatings (figure 3c). Larger water additions promote worse quality films and low growth as can be clearly observed in figure 3d. In fact this phenomenon of a window for the homogeneous deposition conditions has been previously observed by other authors for other polar/non-polar solvent mixtures [37, 52, 53].

Although water addition promotes a slightly film growth, the achievement of homogeneous films concurs within the interval of higher deposited mass observed in figure 3a. Therefore, suspension stability evidenced by the film homogeneity is also noticeable through the relative increase of the deposition rate. The stability of the suspension is associated to two phenomena. One is the particle deagglomeration, which is related to the film homogeneity, and the other is the particle electrokinetics where faster particles lead to higher deposited mass. For that reason a narrow range of stability could be determined where homogeneous and heavier coatings can be produced.

Obvious Labib et al. [16] have studied the donor-acceptor behaviour of organic solvent with oxides, suggesting that particles acquire their charge from direct electron transfer from a neutral liquid molecule in most cases. The donor-acceptor role depends on the electron donicity of the solvent linked to the particle. Some publications dealing with EPD films report the dispersion of several particles in acetone. In these works, oxides (such as SiO_2) in which acid sites predominate at the surface develop a negative charge in acetone dispersions [19, 33, 35, 51, 60]. Since the solvent acts as donor, electron transfer occurs from the liquid to the solid. Oxides such as ZrO_2 show a zero surface charge in acetone [52, 53, 61], while other oxides, i.e. ZnO, MgO, SbO, etc., behave as positive particles depositing in the cathode [62-67]. In later cases, electron transfer occurs from solid to liquid, having the solvent a lower donicity character than considered oxides. Similarly occurs for the SbO or PZT when inorganic bases or acids, i.e. NH_4OH and HNO_3, were added in acetone [66-68] or alcoholic media [59, 68, 69].

In 0.1 g/l suspensions in dry acetone, the solvent acts as donor, and electron transfer takes place from the liquid to the solid leading to negative surfaces. In acetone-water mixtures, the presence of water steps up YBCO dissolution and $BaCO_3$ formation. Since YBCO dissolution occurs in a lower ratio than in aqueous suspensions, protons liberated by the Ba^{+2} carbonation (figure 1) promote the acetone protonation, displacing the equilibrium through the enol formation [70]. In this case, the change in the donor-aceptor character of the solvent is the main cause of the evolution of the YBCO charged surfaces. This behaviour is more evident for concentrated suspensions, where YBCO particles have higher zeta potentials leading to a clear cathodic deposition.

Moreover, the adsorption of water at the particle surface increases its donicity, helping to charge transfer [55]. Hence, larger amounts of water enhance charging and improve the uniformity of the coatings, as seen in figure 3c. The presence of ions produced by the YBCO dissolution in 10 g/l suspensions fits the increase of conductivity. If the amount of water is larger the charging mechanism by selective adsorption of ions (H^+, Ba^{2+} and $Ba(OH)^+$) on hydrated surfaces [18] should displace

the donor-acceptor mechanism. In those cases, stability conditions should be studied and adjusted, because of those YBCO suspensions lead to heterogeneous deposits (figure 3d).

Finally, although homogeneous YBCO films can be achieved with water as dispersing agent, stability attained through above described mechanisms depends on the weak chemical stability of YBCO surfaces, which can jeopardize process reliability. In view of these results further studies considering other stabilisers combined with water should be developed.

3.2. Dispersing mechanism of YBCO particles in acetone-I_2 solution

Early studies dealing with structures formed by halogen molecules with oxygenated solvents reveal the presence of 1:1 complexes in solutions of iodine in alcohols and ketones, corresponding to the form: $RR'O^+ \cdot I_2^-$ or $RR'CO^+ \cdot I_2^-$ [71]. Complexes result from an acid-base interaction in the electron–donor sense in which iodine acts as the acid or electron-acceptor. The increase of Lewis basicity of the organic oxygenated solvents leads to a high interaction with iodine. Recently, Kebede at al. [72] has demonstrated that solvent-I_2 complex remains in equilibrium with a charged complex form while generates triiodine (I_3^-). The increase of the solution conductivity and the shift to shorter wavelength of the absorption peak of I_2 in the visible region (usually at 500 nm), evidence the presence of the solvent$\cdot I_2$ complex, which later promotes the formation of cationic solvent$\cdot I^+$ complex and I_3^- [72]. Proposed reactions of the I_2 solutions in acetone are:

$$(CH_3)_2CO + I_2 \leftrightarrow (CH_3)_2CO^+ \cdot I_2^- \quad (3)$$

$$(CH_3)_2CO^+ \cdot I_2^- \rightarrow CH_3CH_2ICOH^+ + I^- \quad (4)$$

$$(CH_3)_2CO^+ \cdot I_2^- + I^- \rightarrow (CH_3)_2CO + I_3^- \quad (5)$$

$$I_2^- + I^- \rightarrow I_3^- \quad (6)$$

where reaction (4) summarised the acetone halogenation catalysed by the presence of H_2O, which results in the formation of a stable cation $CH_3CH_2ICOH^+$ [70].

The evolution of specific conductivity with time of technical grade acetone solutions of different I_2 concentrations (0.1, 0.2, 0.4 and 1.0 g/l) is plotted in figure 4a. A sharp increase of conductivity takes place after a certain time for any iodine concentration. This gap is higher and takes place faster as the concentration of I_2 increases. Solution conductivity rises from 50 µS/cm for 0.1 g/l of I_2 to 325 µS/cm at the 1g/l of I_2 solution. These data are in good agreement with those reported in the literature [20].

In addition to specific conductivity measurements, UV/absorbance has been measured for all considered iodine concentrations. Figure 4b shows the evolution of absorbance spectra of solution of 0.2 g/l I_2 in acetone. The maximum absorption is located at 449 nm and is due to polarization of I_2 molecules, as reported by Kebede et al. [72]. During 20 minutes, I_2 adsorption maintains constant. Then, absorbance between 350 and 400 nm grows quickly after about 25 min while the peak at 450 nm disappears. This phenomenon happens simultaneously with the increase of conductivity (figure 4a). I^- absorption is located below 300 nm and could not be responsible of this double effect. The occurrence of species absorbing between 350 and 400 nm is related to I_3^-. Hence, the formation of I_3^- through equations 4, 5 and 6, verified by the UV spectra, becomes associated to the conductivity increase of I_2 solutions in acetone. After complete I_2 dissolution, the ionic species responsible for the high conductivity are the products of equations 4-5: I_3^- and $CH_3CH_2ICOH^+$.

The pH of 0.1, 1 and 10 g/l YBCO suspensions in technical grade acetone with 0.2 g/l of I_2 are plotted in figure 5. YBCO powders were added to the solution of I_2 in

acetone, and then starting pH of suspensions indicates the I_2 acid character [57]. Acidification when increasing concentration of I_2 has been reported in the literature for YBCO in acetone [20] and YSZ in isopropanol or a mixture of acetone and ethanol [50, 52].

The starting pH of 0.1 and 1 g/l YBCO suspensions are by 4.5, while the concentrated suspension shows a pH close to 6. Moreover, the pH of 1 and 10 g/l suspensions slowly increases with time, while in the diluted suspension pH roughly maintains during 40 min.

Surface reactions in YBCO powders also determine the dispersing conditions in I_2-acetone solution. When powder is added, the acidic medium promotes the YBCO dissolution being this effect more evident as solid concentration increases. In fact, Ba^{2+} concentration has been determined by ICP at the supernatant of 10 g/l suspensions being $[Ba^{2+}] = 2\ 10^{-2}$ mol/l. The YBCO surface reaction with solvent promotes neutralization (fig. 5), and then dissolved ions [18], i.e. Ba^{2+}, join ionic species coming from I_2 dissolution (I_3^- and $CH_3CH_2ICOH^+$).

Suspensions of 0.1 g/l of YBCO were prepared in solutions of I_2 in technical grade acetone to determine surface charges. The variation of zeta potential and conductivity with iodine content is represented in figure 6. Conductivity increases linearly with I_2 content. Conductivity values at such low solid contents are similar to those registered for iodine solutions in figure 4a, suggesting that the formation of triodine and $CH_3CH_2ICOH^+$ ions after I_2 dissolution (equations 4-6) results in the largest contribution to the conductivity of 0.1 g/l YBCO suspensions. However, lower conductivity values have been also reported [10, 20] for 10 g/l YBCO suspensions prepared with similar amounts of I_2. Actually, charged particles should increase the number of conductive species in the suspension contributing to increase its conductivity [1, 73]. However, reported results for concentrated suspensions [10, 20] verified the decrease of conductivity with the addition of YBCO particles. Considering the ionic species solved in the suspension (Ba^{2+}, I_3^- and $CH_3CH_2ICOH^+$) the formation of $Ba(I_3)_2$ [74] could be the cause of the suspension conductivity decrease. Concluding that solid-solvent reactivity reduces or inhibits the presence of some ionic species solved in the suspension medium.

The behaviour of zeta potential vs the I_2 content of the solvent is similar to that described in the literature for YBCO [20] and YSZ [45, 49-53] suspensions in different organic solutions of I_2. Zeta Potential is strongly negative (-43 mV) in suspensions without I_2, fitting results plotted in figure 2, while a small amount of I_2 develops positive zeta potentials. A maximum value (+40 mV) was achieved with 0.04 g/l of I_2, while zeta potential maintains constant for further I_2 additions.

The stability of the suspension in technical grade acetone without and with 0.2 g/l iodine has been also qualitatively evaluated by settling tests, plotted in figure 7 for 10 g/l YBCO suspensions. Suspensions prepared in acetone sediment faster, powders being completely settling in 10 minutes. Addition of 0.2 g/l of iodine increases the suspension stability to several hours, although both suspensions, without I_2 and with 0.2 g/l of I_2, have high positive zeta potential values ~30 mV (plots in figure 2, curve a, and 6). Since zeta potential only reflects electrostatic stabilisation, a low sedimentation suggests the presence of steric dispersive forces acting with the I_2 addition, which contributes to suspension stability enhancement.

In order to explain differences in the settling behaviour, the interparticle potentials acting between particles have been modelized. The Derjaguin, Landau, Verwey and Overbeck (DLVO) theory was used. In the case of the suspension without I_2, the electrostatic stabilization is only considered. Therefore the total interaction

potential is determined by electrostatic interactions (V_a and V_r matt addend). However, when I_2 is added, results suggest that an electrosteric stabilization mechanism acts between YBCO particles. In this case, the interparticle interaction potential was calculated considering the attractive (V_a), repulsive (V_r) and steric (V_{ste}) effects. The attractive stabilization (V_a) was approximated by the Gregory's model due to the particle size [75].

$$V_a(d) = -\frac{A_H a}{12d}\left[1 - \frac{bd}{\lambda_0}\ln\left(1 + \frac{\lambda_0}{bd}\right)\right] \quad (7)$$

where a is the particle radius, d is the distance between particles, A_H is the Hamaker constant, λ_0 and b are constants.

The spectral parameters of YBCO and acetone, such as the refractive index, n, and the characteristic adsorption frequency, ω, have been considered to determine the Hamaker constant [76, 77]. The refractive index (n_{AC}) and the characteristic absorption UV frequency (ω_{AC}) of the acetone are 1.36 and 189 nm, respectively [70]. However, when 0.2 g/l I_2 has been dissolved in the acetone, the maximum absorption UV frequency of the liquid medium ($\omega_{AC/I2}$) is ~ 400 nm (figure 4b) [72]. A characteristic absorption frequency in the UV range of 300 nm (ω_{YBCO}) and a related refractive index of 1.69 (n_{YBCO}) have been considered for YBCO particles [78-80], neglecting the anisotropy of its optic and dielectric functions [81]. The Hamaker constant calculated for this approximation results on $4.73\ 10^{-21}$.

The Hogg-Healy-Fuerstenau (HHF) theory, that considered a constant surface charge, was selected to calculate the repulsive electrostatic interaction:

$$V_r(d) = \pi\varepsilon\varepsilon_0 \frac{a}{2} \blacksquare 4\psi^2 \ln(1 + \exp(-\kappa d)) \quad (8)$$

where a is the particles radius, ψ is the surface potential, ε_0 is dielectric constant, ε is the electric constant and y κ is the inverse Debye length. Finally, the simple hard wall model described by Bergström [82] was used to approximate the steric stabilization in the YBCO suspension stabilised in I_2 solution, by means:

$$V_s(d) =: \frac{\pi a k T}{V^3}\Phi^2\left(\frac{1}{2} - \chi\right)(2\delta + 2a - d)^2 \quad (9)$$

δ represents the thickness of the adsorbed layer, Φ the volume fraction of the adsorbent in the adsorbed layer, χ is the solvent-adsorbent interaction parameter and V is the molecular volume solvent. This equation is valid in the interpenetrational domain ($\delta < (D - 2d) < 2\delta$) [82].

As it is discussed above, particles are positive in charge in both suspensions while solved ionic species are different in nature and concentration. In acetone, the conductivity of the YBCO suspension is very low (< 0.2 μS/cm), so the concentration of both co-ions and counter-ions can be also considered low. The operational pH changes towards acid values (ΔpH = 1), pointing up a slightly YBCO dissolution and subsequence quickly Ba^{2+} carbonation. Attending to the pH, only an excess of OH^- ions remains in the suspension (figure 1). Hence, further calculations have been done considering the operational pH in figure 1 to determine the concentration of the only positive ionic specie, i.e. $[H^+]=10^{-8.5}$ mol/l.

It has been also verified that conductivity measured in 0.2 g/l I_2 dissolution in acetone (75 μS/cm in figure 4a) is mainly due to the presence of I_3^- and $CH_3CH_2ICOH^+$ species. However, when YBCO is added, it dissolves leading to the Ba^{2+} leaching and later $Ba(I_3)_2$ precipitation. In this case, the presence of the YBCO, and related surface

reactions, determines the pH (figure 5) and the conductivity of the suspension [10]. Besides species solved due to the acetone halogenation, the main positive ionic species are Ba^{2+} and H^+. As determined above, Ba^{2+} concentration in this suspension is $[Ba^{2+}] = 2\ 10^{-2}$ mol/l. Operational pH is 4 in figure 5, so the H^+ concentration is $[H^+] = 10^{-4}$ mol/l. Consequently, further calculation has been made considering Ba^{2+} as the only co-ion due to its valence (z = +2) and in view of Ba^{2+} concentration is two orders of magnitude higher than H^+ concentration. It is important to note that mistakes done by considering the operational pH, contribute to maximize H^+ concentration in both suspensions (equation 2) [83].

Figure 8 shows the calculated interparticle potential for 10 g/l YBCO suspensions prepared in technical acetone (2.5 vol.% H_2O) (solid line), which presents a primary minimum at short interparticle distances. The energy barrier localizes between 0.5 and 1.5 nm, preventing the attraction between particles. High values of potential interaction at the energy barrier is mainly due to high particle size (4 μm), suggesting that particle coagulation should be avoided for distances higher than 1.5 nm. Consequently, the adsorption of short organic molecules onto the particle surface should be enough to stabilize YBCO suspensions by means a steric mechanism.

Besides positive species solved in presence of 0.2 g/l of I_2, $CH_3CH_2ICOH^+$ can be adsorbed onto the particle surface fitting the characteristic curve of the reversal zeta potential sign in figure 6. Considering an adsorbed layer of 1 nm [84], dot line in figure 8 shows the total interaction potential for 10 g/l YBCO suspensions prepared in 0.2 g/l I_2-acetone solution. The primary minimum disappears since the adsorption of the molecules avoids the direct contact between particles, and the barrier energy moves to 2-2.5 nm. Hence, suspension stability increases justifying settling results in figure 7. The addition of I_2 avoids powder sedimentation for 9 h.

Figure 9a shows the evolution of deposited mass per unit area with increasing I_2 contents in 10 g/l YBCO suspensions in technical grade acetone. EPD tests were carried out applying 200 V for 60 s. The film growth with water addition (figure 3a), under similar electric conditions (200 V) for 180 s, has been also plotted for comparative proposes. Particle migration always occurs toward the negative electrode (cathode) with I_2, as expected from positive zeta potential values of YBCO (figure 2, curve b, and figure 6). Deposit growths homogeneously compared to low reliability and uniformity of deposits without I_2. Maximum deposition takes place for 0.04-0.05 g/l of I_2, while a larger addition of I_2 (>0.15 g/l) reduces the deposit yield because of higher suspension conductivities [10, 73].

In agreement with other authors (table 1), deposition with I_2 as stabilizer achieves a maximum fitting higher zeta potential values. A picture of a deposit obtained applying 200V for 60 s in a 10 g/l suspension in 0.2 g/l of I_2 acetone solution was shown in figure 9b.

Finally, I_2 plays an important role in the charging mechanism of the YBCO surfaces. The stability in acetone without I_2 depends on the donor-acceptor character of the pair powder-solvent, while an optimal I_2 content assures suspension stability, enhancing film growth in terms of higher reliability, homogeneity and deposit yield.

The interaction of I_2 with solvents depends on their basic character. Detailed studies summarized in table 1 suggest that dispersion with I_2 is more effective in solvents mainly composed by ketones. A recent study demonstrates that dispersion depends on the I_2-solvent interaction [37], while results in table 1 verify that the amount of I_2 for each system solvent-particle should be optimised. In fact, the surface charge of the particles becomes positive whatever was their nature [19, 33-44], and the effective amount of I_2 added is related to the morphologic properties of the particles [38, 58, 85].

In the case of acetone, the effectiveness of I_2 as stabilizing agent should be mainly attributed to the formation of the iodine complex cation $CH_3CH_2ICOH^+$ in acetone solutions (equations 3-6). This ion adsorbs onto YBCO surfaces leading to a positive charge. Moreover, according to the stabilization mechanisms proposed for organic media [86], the presence of a small amount of water (2.5 vol.% in technical grade acetone) helps to the $CH_3CH_2ICOH^+$ adsorption. This assures a steric hindrance operating at very short interparticle distances, while the presence of charges provides a high positive zeta potential and hence, the electrostatic repulsion at longer distances shown in the interparticle potential plot in figure 8.

Concluding, the experimental techniques used in this work, including conductivity, pH measurements, zeta potential, settling tests and visible/UV spectra support the proposed charging mechanism. The $CH_3CH_2ICOH^+$ surface adsorption is consistent with the zeta potential plots in figure 6, and those collected in the literature (table I). The steric effect of the $CH_3CH_2ICOH^+$ adsorption contributes to prevent the particles coagulation predicted by the calculated interparticle potential interaction in technical grade acetone (figure 8), and explain the low sedimentation rate of 10 g/l YBCO suspension prepared in a 0.2 g/l I_2 solution in acetone (figure 7). Otherwise, the presence of that organic short chain at the particle surface promotes a higher cohesion between particles and improves particles-substrate adherence leading to a homogeneous and reliable film growth, as shown in figure 9.

4. Conclusions

Charging of YBCO particles in an acetone-I_2 solution has been described. This stabilisation mechanism can be extensive to the dispersion of such a kind of particles in a halogenated organic liquid. The present work states that surface charging in I_2 acetone solution takes place through the formation of $CH_3CH_2ICOH^+$ intermediated complex cations. The adsorption of this species provides a steric contribution to the stabilisation mechanism. Hence an optimal I_2 content assures suspension stability, enhancing film growth in terms of higher reliability, homogeneity and deposit yield..

Specifically, the iodine complex cation $CH_3CH_2ICOH^+$ in YBCO suspensions stabilized by I_2 addition adsorbs onto YBCO surfaces helped by the presence of a small amount of water. This assures a steric hindrance operating at very short interparticle distances, while the presence of charges provides a high positive zeta potential and hence, the electrostatic repulsion at longer distances.

Low chemical stability of YBCO surfaces determines dispersing conditions in acetone, solid and water contents being key parameters for later shaping process. Solid-solvent reactivity determines the number of positive/negative sites at the particle surface. The Ba^{2+} carbonation kinetics determines the keno-enol equilibrium changing the solvent donor-acceptor character, and then the YBCO surface charge. In order to obtain homogeneous YBCO deposits by EPD, 10 g/l suspensions in at least technical grade acetone (2.5 vol.% of water) are desirable.

Acknowledgements

The authors gratefully acknowledge financial support from the Belgian Science Policy (FNRS) under the Interuniversity Attraction Poles programme (INANOMAT - P6/17) and from the Spanish Science and Education Ministry (MEC) through Project MAT2009-14448-C02-01, IPT-310000-2010-12.

References

1. Bersa L, Liu M. A review on fundamentals and applications of electrophoretic deposition (EPD). *Prog Mater Sci* 2007; **52**: 1–61.
2. Boccaccini A, Roether JA, Thomas BJC, Shapper MSP, Chavez E, Stoll E, Minay EJ. The electrophoretic deposition of inorganic nanoscaled materials. *J Ceram Soc Jpn* 2006; **114**: 1-14.
3. Badin J. *Coated conductor technology roadmap - Priority research and development activities leading to economical commercial manufacturing*. ed. Energetics Inc., Oak Ridge National Laboratory, Los Alamos National Laboratory, Argonne National Laboratory; 2001.
4. Bhattacharya R, Phok S, Spagnol P, Chaudhuri T. Electrodeposited biaxially textured buffer layer for $YBa_2Cu_3O_{7-\delta}$ (YBCO) superconductor oxide films. *J Electrochem Soc* 2006; **153**: C273-C276.
5. Su J, Chintamaneni V, Mukhopadhyay M. Photoelectron spectroscopic investigation of transformation of trifluoroacetate precursors into superconducting $YBa_2Cu_3O_{7-x}$ films. Appl Surf Sci 2007; **17**: 4652-4658.
6. Pavese F. Magnetic shielding. In: B. Seeber *editor*. *Handbook of applied superconductivity*, Ginebra: IoP publishing; 1998, pp. 1461-1483.
7. Müller R, Fuchs G, Grahl A, Köhler A. Magnetic shielding properties of $YBa_2Cu_3O_{7-x}$ tubes. *Supercond Sci Technol* 1993; **9**: 225-232.
8. Niculescu H, Schmidmeier R, Topolski B, Gielisse PJ. Shielding effects in ceramic superconductors. *Phys C* 1994; **229**: 105-112.
9. Denis S, Dusoulier L, Dirickx M, Vanderbemden Ph, Cloots R, Ausloos M, Vanderheyden B. Magnetic shielding properties of high-temperature superconducting tubes subjected to axial fields. *Supercond Sci Technol* 2007; **20**: 192-201.
10. Dusoulier L, Denis S, Vanderbemden Ph, Dirickx M, Ausloos M, Cloots R, Vertruyen B. Preparation of $YBa_2Cu_3O_{7-x}$ superconducting thick films by the electrophoretic deposition method. *J Mater Sci* 2006; **41**: 8109-8114.
11. Ondoño-Castillo S, Casañ-Pastor N. Deposition of $YBa_2Cu_3O_{7-\delta}$ over metallic substrates by electrophoresis of suspensions in isobutylmethylketone. Influence of electric field, thermal and mechanical treatments. *Phys C* 1996; **268**: 317-33.
12. Soh D, Shan Y, Park J, Li Y, Cho Y. Preparation of YBCO superconducting thick film by electrophoresis. *Phys C* 2000; **337**: 44-48.
13. Trolier SE, Atkinson SD, Fuierer PA, Adair JH, Newnham RE. Dissolution of $YBa_2Cu_3O_{(7-x)}$ in various solvents. *Am Ceram Soc Bull* 1988; **67** (4): 759-762.
14. Frase KG, Liniger EG, Clarke DR. Environmental and solvent effects on yttrium barium cuprate ($Y_1Ba_2Cu_3O_X$). *Adv Ceram Mat* 1987; **2**: 698-700.
15. Barkat A, Hojaji H, Michael KA. Reactions of barium yttrium copper oxides with aqueous-media and their applications in structural characterization. *Adv Ceram Mat* 1987; ***2***: 701-709.
16. Labib ME, Zanzucchi PJ. The use of Zeta-Potential measurements in organic solvents to determine the donor-acceptor properties of solid surfaces. *Inter Phen Biotech Mat Proc* 1988; **97**: 139-148.
17. Komori K, Kozuka H, Saca S. Chemical durability of a superconducting oxide $YBa_2Cu_3O_{7-x}$ in aqueous-solutions of varying ph values. *J Mat Sci* 1989; **24**: 1889-1894.
18. Dusoulier L, Cloots R, Vertruyen B, Garcia-Fierro JL, Moreno R, Ferrari B, *Mater Chem Phys* 2009; **116**: 368–375.

19. Takayama Y, Negishi H, Nakamura S, Koura N, Idemoto Y, Yamaguchi F. Zeta potential of various oxide particles and the charging mechanism. *J Ceram Soc Jpn* 1999; **107**: 119-122.
20. Koura N, Tsukamoto T, Shoji H, Hotta T. Preparation of various oxides films bv an electrophoretic method: a study of the mechanism. *Jpn J Appl Phys* 1995; **34**: 1643-1647.
21. Cho S, Tao YT, Ketterson JB. J_c enhancement of electrophoretically deposited $YBa_2Cu_3O_{7-x}$ superconducting wire by BaF_2 addition. *Appl Phys Lett* 1995; **67** (6): 851-853.
22. Nojima H, Shintaku H, Nagata M, Koba M. Fabrication of Ag-doped $Y_1Ba_2Cu_3O_{7-x}$ superconducting films on cu substrates by electrophoretic deposition. *Jpn J Appl Phys* 1991; **30** (7): L1166-L1168.
23. Zhang B, Fabbricatore P, Gemme G, Musenich R, Parodi R, Risso L. Preparation and characterization of $YBa_2Cu_3O_{7-x}$ superconducting films deposited by electrophoresis. *Phys C* 1992: **193**: 1-7.
24. Fujimoto M, Nojima H, Shintaku H, Taniguchi H, Nagata M, Koba M. Study of Ag addition to $YBa_2Cu_3O_{7-x}$ films prepared using electrophoretic deposition. *Jpn J Appl Phys* 1993; **32**: L576-L579.
25. Chu CY, Dunn B. Fabrication of $YBa_2Cu_3O_{7-x}$ superconducting coatings by electrophoretic deposition. *Appl Phys Lett* 1989; **55**: 492-494.
26. Wang J, Maloufi N, Xue XX, Fan ZG, Esling C. Textured YBaCuO films enhanced by cold rolling and melt growth process in low oxygen partial pressure. *Solid State Phenomena* 2005; **105**: 453-458.
27. Zhu YB, Zhou YL, Liu Z, Wang SF, Chen ZH, Lu HB, Yang GZ, Xiao L, Ren HT, Jiao YL, Zheng MH. Critical current density enhancement of electrophoretically deposited Y-Ba-Cu-O superconducting coating by annealing in high pressure oxygen. *Phys C* 2004; **403**: 172-176.
28. Kawachi M, Sato N, Suzuki E, Ogawa S, Noto K, Yoshizawa M. Fabrication of $YBa_2Cu_3O_{7-x}$ films by electrophoretic deposition technique. *Phys C* 2001; **357-360**: 1023-1026.
29. Sato N, Kawachi M, Noto K, Yoshimoto N, Yoshizawa M. Effect of particle size reduction on crack formation in electrophoretically deposited YBCO films. *Phys C* 2001; **357-360**: 1019-1022.
30. Niu H, Shikawata H, Hagiwara Y, Kishino S. Fabrication of Y-Ba-Cu-O superconducting films by electrophoresis with the use of firing in helium ambience. *Supercond Sci Tech* 1991; **4**: 229-231.
31. Ochsenkühn-Petropulu O, Tarantilis P, Tsarouchis J, Ochsenkühn K, Parissakis G. Optimization of the electrophoretic deposition of $YBa_2Cu_3O_{7-x}$ superconducting large area coatings. *Mikrochim Acta* 1998; **129**: 233-238.
32. Das-Sharma A, Sen A, Maiti HS. Effectiveness of various suspension media for electrophoretic deposition of YBCO superconductor powder. *Ceram Inter* 1993; **19**: 65-70.
33. Fukuda H, Matsumoto Y. Formation of Ti–Si composite oxide films on Mg–Al–Zn alloy by electrophoretic deposition and anodisation. *Electrochim Acta* 2005; **50**: 5329–5333.
34. Matsuda M, Higashi Y, Tadanaga K, Minami T, Tatsumisago M. Electrophoretic Deposition of Sol-Gel derived V_2O_5 microparticles and its application for cathodes for Li-Secondary Batteries. *Key Eng Mater* 2006; **314**: 107-111.

35. Yamaguchia S, Yabutsukab T, Hibinoc M, Yamaguchi TY. Apatite pattern formation by Electrophoretic Deposition transcribing resist pattern. *Key Eng Mater* 2006; **309-311**: 659-662.
36. Peng Z, Liu M. Preparation of dense plattinum-yttria stabilized zirconio and yttria stabilized zirconio film son porous $La_{0.9}Sr_{0.1}MnO_3$ (LSM) substrates. *J Am Ceram Soc* 2001; **84**: 283-288.
37. Aruna ST, Rajam KS. A study on the electrophoretic deposition of 8YSZ coating using mixture of acetone and ethanol solvents. *Mater Chem Phys* 2008; **111**: 131–136.
38. Hyam RS, Subhedar KM, Pawar SH. Effect of particle size distribution and zeta potential on the electrophoretic deposition of boron films. *Colloids Surf, A* 2008; **315**: 61–65.
39. Grinis L, Dor S, Ofir A, Zaban A. Electrophoretic deposition and compression of titania nanoparticle films for dye-sensitized solar cells. *J Photochem Photobiol, A* 2008; **198**: 52–59.
40. Kaya C, Kaya F, Su B, Thomas B, Boccaccini A R. Structural and functional thick ceramic coatings by electrophoretic deposition. *Surf Coat Technol* 2005; **191**: 303–310.
41. Santillán MJ, Quaranta NE, Membrives F, Boccaccini AR. Characterization of TiO_2 nanoparticle suspensions for electrophoretic deposition. *J Nanoparticle Res* 2008; **10**: 787–793.
42. Santillán MJ, Caneiro A, Quaranta N, Boccaccini AR. Electrophoretic deposition of $La_{0.6}Sr_{0.4}Co_{0.8}Fe_{0.2}O_{3-\delta}$ cathodes on $Ce_{0.9}Gd_{0.1}O_{1.95}$ substrates for intermediate temperature solid oxide fuel cell (IT-SOFC). *J Eur Ceram Soc* 2009; **29** (6): 1125-1132.
43. Mathews T, Rabu N, Sellar JR, Muddle BC. Fabrication of $La_{1-x}Sr_xGa_{1-y}Mg_yO_{x-(x+y)/2}$ thin films by electrophoretic deposition and its conductivity measurement. *Solid State Ionics* 2000; **128**: 111–115.
44. Bozza F, Polini R, Traversa E. High performance anode-supported intermediate temperature solid oxide fuel cells (IT-SOFCs) with $La_{0.8}Sr_{0.2}Ga_{0.8}Mg_{0.2}O_{3-\delta}$ electrolyte films prepared by electrophoretic deposition. *Electrochem Commun* 2009; **11** (8): 1680-1683.
45. Ishihara T, Shimose K, Kudo T, Nishiguchi H, Akbay T, Takita Y. Preparation of yttria-stabilized zirconia thin films on strontium-doped $LaMnO_3$ cathode substrates via electrophoretic deposition for solid oxide fuel cells. *J Am Ceram Soc* 2000; **83**: 1921-1927.
46. Kobayashi K, Takahashi I, Shiono M, Dokiya M. Supported $Zr(Sr)O_2$ SOFCs for reduced temperature prepared by electrophoretic deposition. *Solid State Ionics* 2002; **152-153**: 591-596.
47. Matsuda M, Ohara O, Murata K, Ohara S, Fukui T, Miyake M. Electrophoretic fabrication and cell performance of dense Sr- and Mg-dopped $LaGaO_3$-based electrolyte films. *Electrochem Solid-State Lett* 2003; **6**: A140-A143.
48. Argirusis Chr, Damjanovic T, Borchardt G. Electrophoretic deposition of thin SOFC-electrolyte films on porous $La_{0.75}Sr_{0.2}MnO_{3-x}$ cathodes. *Key Eng Mater* 2004; **453-454**: 335-342.
49. Jia L, Lu Z, Huang X, Liu Z, Chen K, Sha X, Li G, Su W. Preparation of YSZ film by EPD and its application in SOFCs. *J Alloys Compd* 2006; **424**: 299-303.
50. Lee YH, Kuo CW, Shih CJ, Hung IM, Fung KZ, Wen SB, Wang MC. Characterization on the electrophoretic deposition of the 8 mol% yttria-

stabilized zirconia nanocrystallites prepared by a sol-gel process, *Mater Sci Eng A* 2007; **445-446**: 347-354.

51. Negishi H, Endo A, Nakaiwa M, Yanagishita H. Preparation of mesoporous Silicate thick films by Electrophoretic Deposition and their adsorption properties of water vapour. *Key Eng Mater* 2006; **314**: 147-152.
52. Chen F, Liu M. Preparation of yttria-stabilized zirconia (YSZ) films on $La_{0.85}Sr_{0.15}MnO_3$ (LSM) and LSM-YSZ substrates using an electrophoretic deposition (EPD) process. *J Eur Ceram Soc* 2001; **21**: 127-134.
53. Yang K, Shen JH, Yang KY, Hung IM, Fung KZ, Wang MC. Characterization of the yttria-stabilized zirconia thin film electrophoretic deposition on $La_{0.85}Sr_{0.15}MnO_3$ substrate., *J Alloys Compd* 2007; **436**: 351-357.
54. Wang Z, Shemilt J, Xiao P. Fabrication of ceramic composite coatings using electrophoretic deposition, reaction bonding and low temperature sintering. *J Eur Ceram Soc* 2002; **22**: 183-189.
55. Parks GA, Bruyn PL. The zero point of charge of oxides. *J Phys Chem* 1962; **66**: 967-973.
56. Zhitomirsky I. Cathodic electrodeposition of ceramic and organoceramic materials. Fundamental aspects. *Adv Coloidl Interface Sci* 2002; **97**: 279-317.
57. Jensen WB. The Lewis acid-base definitions: a status report. *Chem Rev* 1978; **78**: 1-22.
58. Moreno R. The role of slip additives in tape casting technology: Part I-solvents and dispersants. *Am Ceram Soc Bull* 1992; **71**: 1521-1530.
59. Sarkar P, Nicholson PS. Electrophoretic deposition (EPD): mechanisms, kinetics and application to ceramics. *J Am Ceram Soc* 1996; **79** (8): 1987-2002.
60. Kamada K, Mukai M, Matsumoto Y. Electrophoretic deposition assisted by soluble anode. *Mater Lett* 2003; **57**: 2348-2351.
61. Ishiara T, Sato K, Takita Y. Electrophoretic deposition of Y_2O_3-stabilized ZrO_2 electrolyte films in solid oxide fuel cells. *J Am Ceram Soc* 1996; **79**: 913-919.
62. Hosseinbabaei F, Taghibakhsh F. Electrophoretically deposited zinc oxide thick film gas sensor. *Electron Mater Lett* 2000; **36**: 1815-1816.
63. Hosseinbabaei F, Raissidehkordi B. Electrophoretic deposition of MgO thick films from an acetone suspension. *J Eur Ceram Soc* 2000; **20**: 2165-2168.
64. Negishi H, Sakai N, Yamaji K, Horita T, Yokokawa H. Application of Electrophoretic Deposition Technique to Solid Oxide Fuel Cells. *J Electrochem Soc* 2000; **147**: 1682-1687.
65. Chang J, Jang E, Sohn B, Hwang S, Choy J. High-Tc superconducting thin film from bismuth cuprate nano-colloids. *Thin Solid Films* 2006; **495**: 78-81.
66. Kuwabara K, Nora Y. Electrophoretic preparation of antimonio acid film. *J Mater Sci* 1993; **28**: 5257-5261.
67. Sweeney TG, Whatmore RW. Electrophoretic deposition of ferroelectric thin films. *Ferroelectrics* 1996; **187**: 53-57.
68. Widegren J, Bergström L. The effect of acids and bases on the dispersion and stabilization of ceramic particles in ethanol. *J Eur Ceram Soc* 2000; **20**: 659-665.
69. Damodaran R, Moudgil BM. Electrophoretic deposition of calcium phosphates from non-aqueous media. *Colloids Surf., A* 1993; **80**: 191-195.
70. Morrison RT. *Organic Chemistry*, Boston: Fondo Educativo Interamericano, S.A; 1973.
71. Mulliken RS. Structures of complexes formed by halogen molecules with aromatic and with oxygenated solvents. *J Am Chem Soc* 1950; **72**: 600-608.

72. Kebede Z, Lindquist SE. Donor-acceptor interaction between non-aqueous solvents and I_2 to generate I_3^-, and its implication in dye sensitized solar cells. *Sol Energy Mater Sol Cells* 1999; **57**: 259-275.
73. Ferrari B, Moreno R. Electrophoretic Deposition of Aqueous Alumina Slips. *J Eur Ceram Soc* 1997; **17**: 549-556.
74. Pearce JN, Eversole WG. The equilibrium between Iodine and Barium Iodide in aqueous solutions. *J Phys Chem* 1924; **28** (3): 245-255.
75. Bowen WR, Jenner F. The calculation of the dispersion forces for engineering applications. *Adv Colloid Interface Sci* 1995; **56**: 201-243.
76. Bergstrom L. Hamaker constants of inorganic materials. Adv Colloid Interface Sci 1997; **70**: 125-169.
77. Bergstrom L, Meurk A, Arwin H, Rowcliffe D. Estimation of Hamaker constants of ceramic materials from optical data using Lifshitz theory. *J Am Ceram Soc* 1996; **79** (2): 339-348.
78. Branescu M, Vailionis A, Gartner M, Anastasescu M. Spectroscopic and X-ray diffraction study of high Tc epitaxial YBCO thin films obtained by pulsed laser deposition. *Appl Surf Sci* 2006; **253**: 400–404.
79. Michaelis A, Irene EA, Auciello O, Krauss AR, Veal B. A spectroscopic anisotropy ellipsometry study of $YBa_2Cu_3O_{7-y}$ superconductors. *Thin Solid Films* 1998; **313-314**: 362-367.
80. Kezuka H, Masaki T, Hosokawa N, Hirata K, Ishibashi K. Refractive index of high-Tc YBCO superconductors. *Phys C* 1991; **185-189**: 999-1000.
81. Lue JT, Nee TW, Chu JJ, Chang CM. Electronic structure and optical spectra of $YBa_2Cu_30_{7-y}$ thin films in the infrared and UV region. *Appl Phys A: Mater Sci Process* 1992; **55**: 192-195.
82. Bergström L, Schilling C H, Aksay I A. Consolidation behaviour of flocculate alumina suspensions. *J Am Ceram Soc* 1992; **75** (12): 3305-3314.
83. Palit SR, Das MN, Somayajulu GR. *Non-aqueous titration. A monograph on acid-base titration in organic solvents*, Calcuta: Indian Association for Cultivation of Science; 1954.
84. Chu Q, Bonnamy S, Van Damme H. Surface and colloidal properties of silica fumes in aqueous medium. In Malhotra VM, editor. *Fly ash, silica fume, slag and natural pozzolans in concrete proceedings of the 5th International conference*, Detroit: Amer Cocrete Inst; 1995, pp. 135-138.
85. Cesarano J, Aksay IA. Processing of highly concentrated aqueous alpha-alumina suspensions stabilized with poly-electrolytes. *J Am Ceram Soc* 1988; **71**: 1062-1067.
86. Fowkes, F.M., Dispersions of ceramic powders in organic media. In Messing GL, Mazdeyashi KS, McCauley JW, Haber RA, editors. *Advances in ceramics, vol 21: Ceramic Powder Science*, Westerville: The Am Ceram Soc Inc; 1987, pp. 411-421.

Table 1. Data collected from published dispersing studies of oxide particles in organic solvents with I_2. The nature, size, and specific surface area (SSA) of the particles, solid content, solvent, pH, specific conductivity (σ), I_2 content, zeta potential (ZP) of the suspensions, and mass per unit area deposited (m) under determined electrical conditions (EC) are shown.

Ref	PARTICLE			SUSPENSION						EPD	
	Oxides	Size *μm*	SSA *m^2/g*	Solids *g/l*	Solvent	pH[a]	σ[b] mS/cm	I_2[c] *g/l*	ZP[d] *mV*	m[d] *mg/cm^2*	EC *V x min*
[49]	YSZ	0.25	12	10	IPA	-	-	0.5	+15	60-65	10 x 60
[50]	YSZ	0.25	12	10	IPA	6-2	-	0.6	+40	-	-
		0.008	117	10	IPA	7-2	-	0.2	+35	4	10 x 20
[52]	YSZ	0.25	12	9	EtOH	-	-	0.4	+20	-	-
					Ac	-	-	0.4	+65	-	-
					AcAc	-	-	0.4	+45	-	-
					Ac/EtOH	7-2	<14	0.4	+60	12	20 x 8
[53]	YSZ	0.25	12	2	Ac/EtOH	-	-	0.6	+45	1	10 x 1
[45]	YSZ	0.25	12	10	AcAc		<12	0.5	+50	65	10 x 20
[12]	YBCO	1-5	-	10	Ac	-	-	-	-	50	-
[20]	YBCO	-	-	10	Ac	3-4	< 0.2	1	+65	4	150 x 0.5
	BT	-	-	10	Ac	-	-	0.5	+70	-	-
[10]	YBCO	2-6	-	10	Ac	-	< 0.13	-	-	-	-

[a] pH range from suspensions prepared adding I_2 up to 1 g/l
[b] Conductivity measured for suspension prepared adding I_2 up to 1 g/l.
[c] I_2 concentration of the suspensions with maximum zeta potential and for a maximum in the deposited mass
[d] Maximum zeta potential and mass per unit area deposited under described electrical conditions related to a I_2 concentration.

Table 2: Electrophoretic migration and deposition sense related to the suspensions solid contents and the solvent analytical grade.

Acetone grade	**0.1 g/l**	**1 g/l**	**10 g/l**
Technical	Anodic	Cathodic	Cathodic
Dry	Anodic	Cathodic	Cathodic

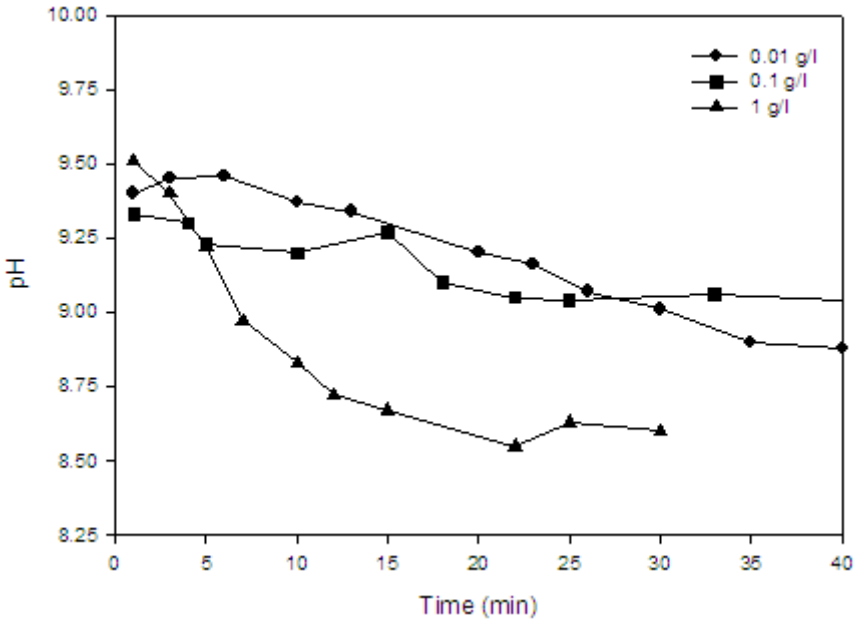

Figure 1. Evolution of pH for suspensions in technical grade acetone with 0.1, 1 and 10 g/l YBCO concentrations.

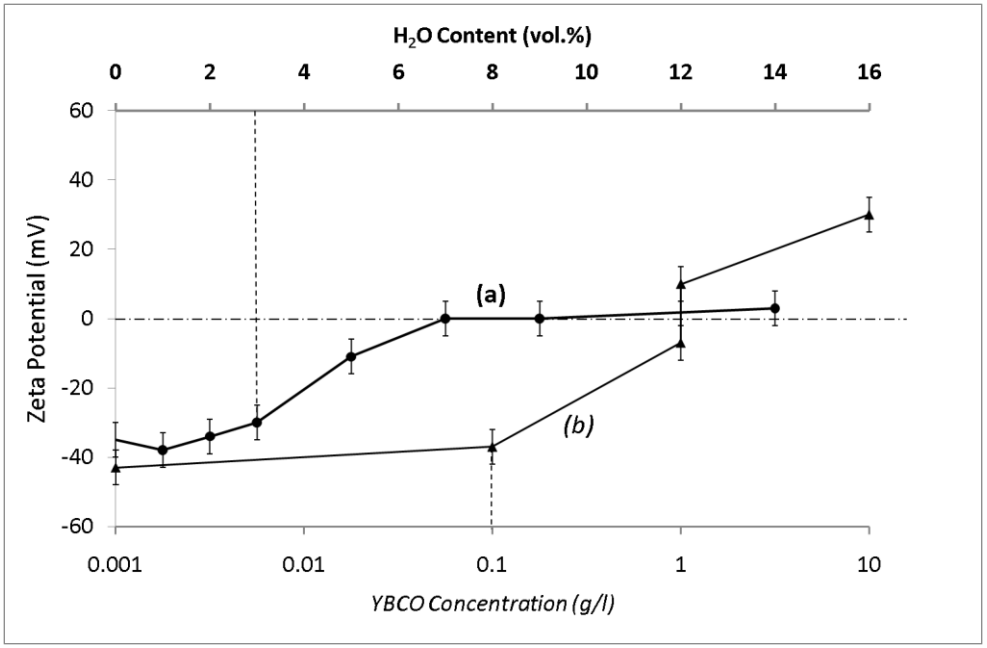

Figure 2. Zeta potential of YBCO suspensions prepared:

- *curve (a)*, in dry acetone with a solid content of 0.1 g/l, related to the added amount of water, and
- *curve (b)*, in technical grade acetone (~2.5 vol.% of water), related to the solids concentration increase.

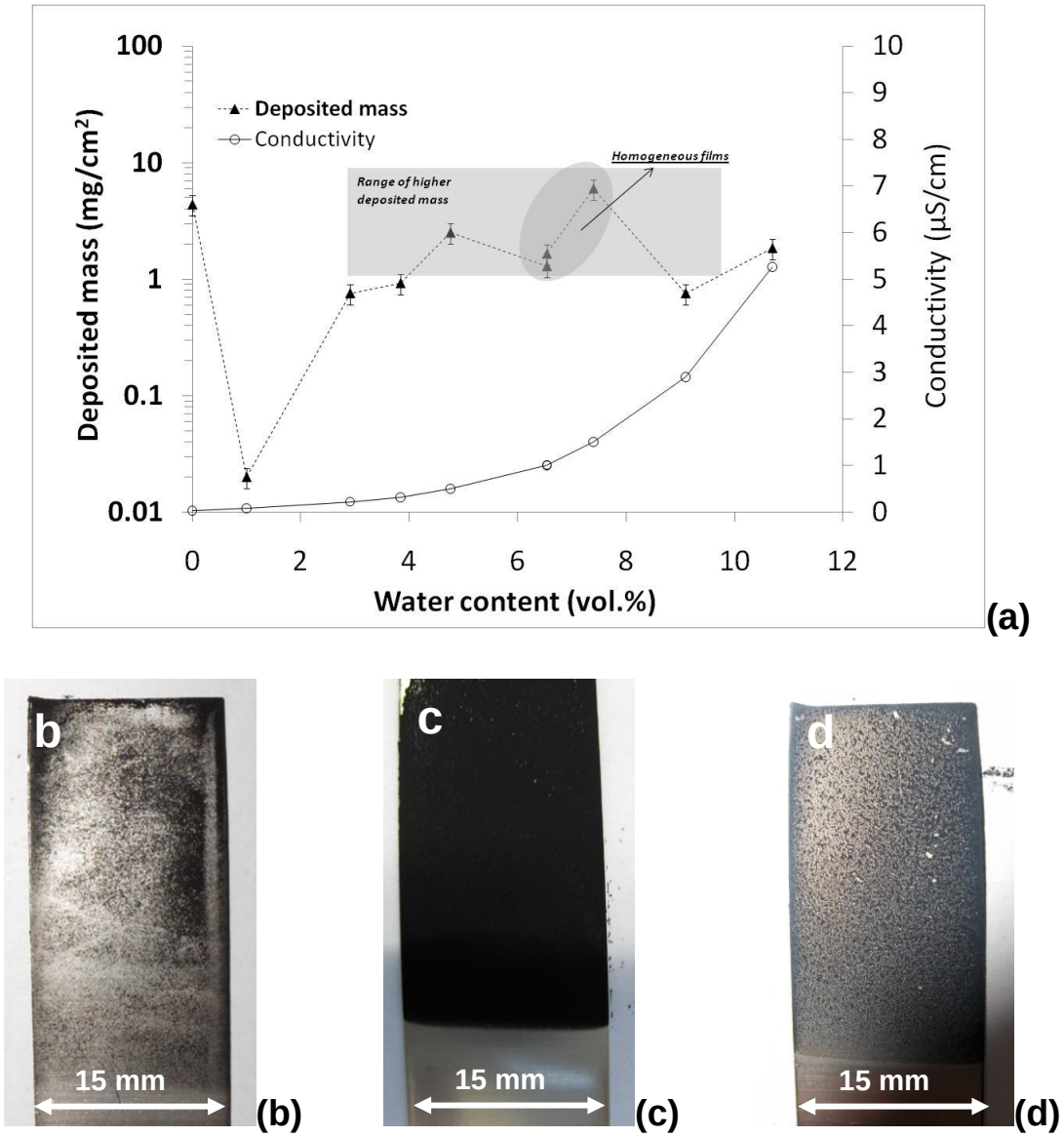

Figure 3. (a) Deposited mass and suspension conductivity as a function of the water content for 10 g/l suspensions in acetone. YBCO coatings obtained by EPD using 10 g/l suspensions prepared in acetone with 2.9 (b), 6.5 (c) and 10.7 (d) vol% of water.

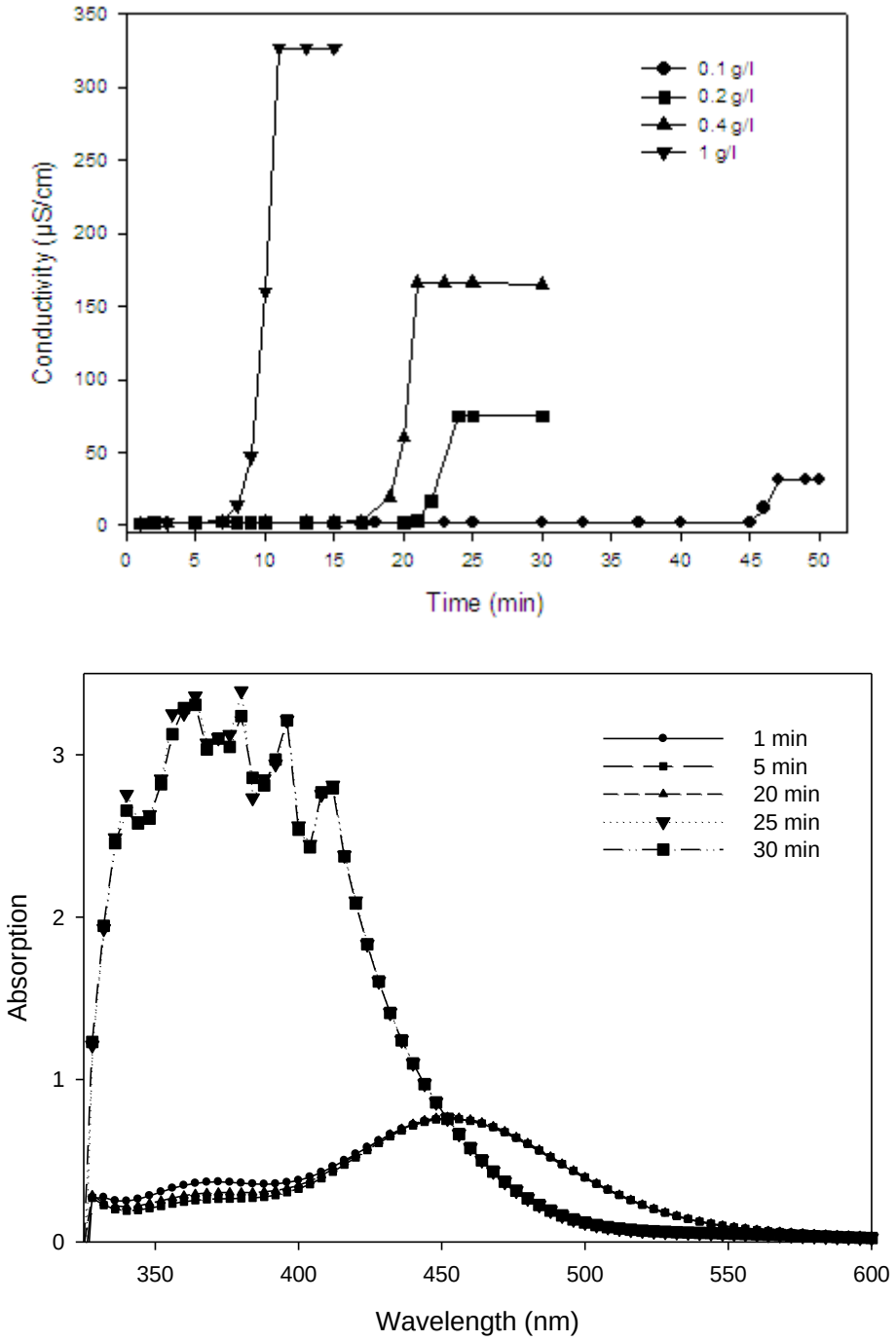

Figure 4. (a) Specific conductivity evolution with time for different I_2 concentrations in acetone. (b) UV/Visible spectra evolution with time in a solution of 0.2 g/l of iodine in acetone.

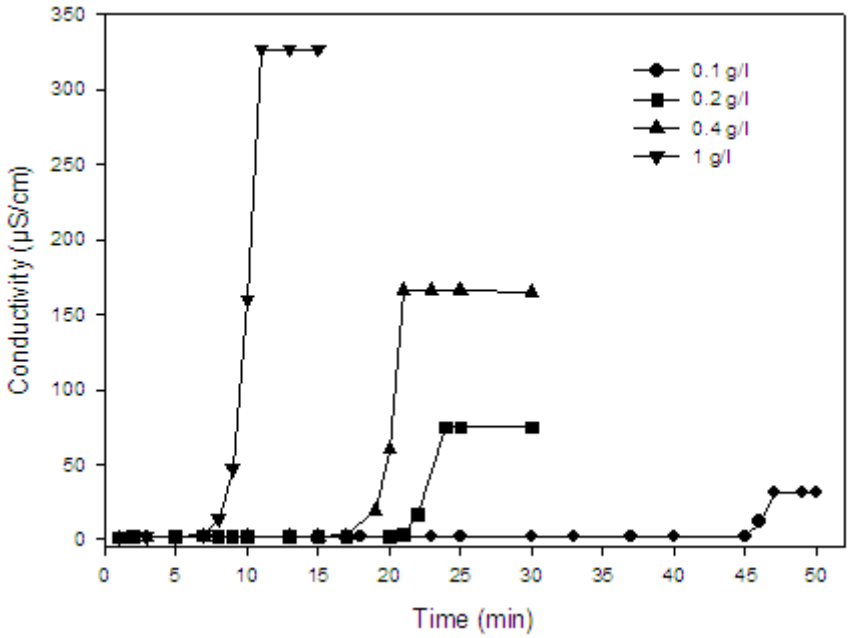

Figure 5. Evolution of operational pH for suspensions of different amounts of YBCO in a solution of 0.2 g/l I_2 in acetone.

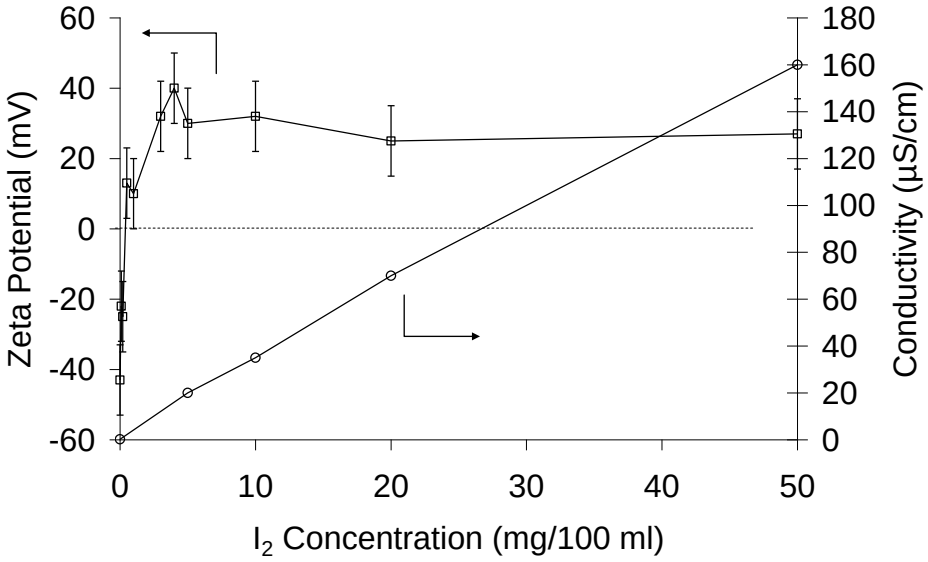

Figure 6. Zeta potential and specific conductivity with iodine content

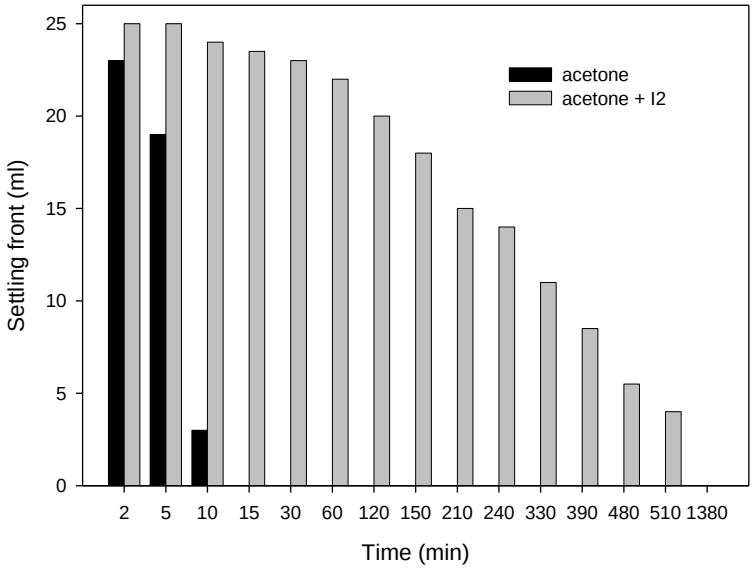

Figure 7. Sedimentation behaviour of acetone suspension with and without iodine.

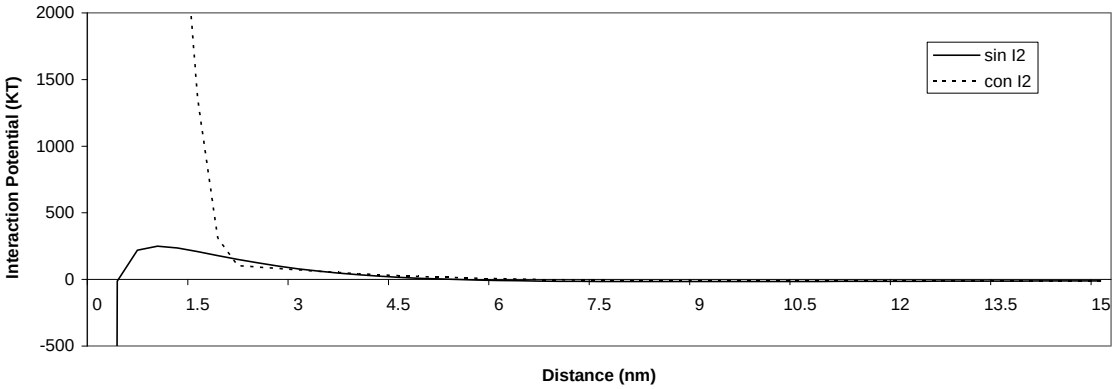

Figure 8. Interaction potentials for 10 g/l YBCO suspensions prepared in technical grade acetone (—) and a 0.2 g/l I_2 solution in acetone (- - -) .

Published in: Journal of the European Ceramic Society (2011), vol. 31, pp. 1075-1086.
Status: Postprint (Author's version)

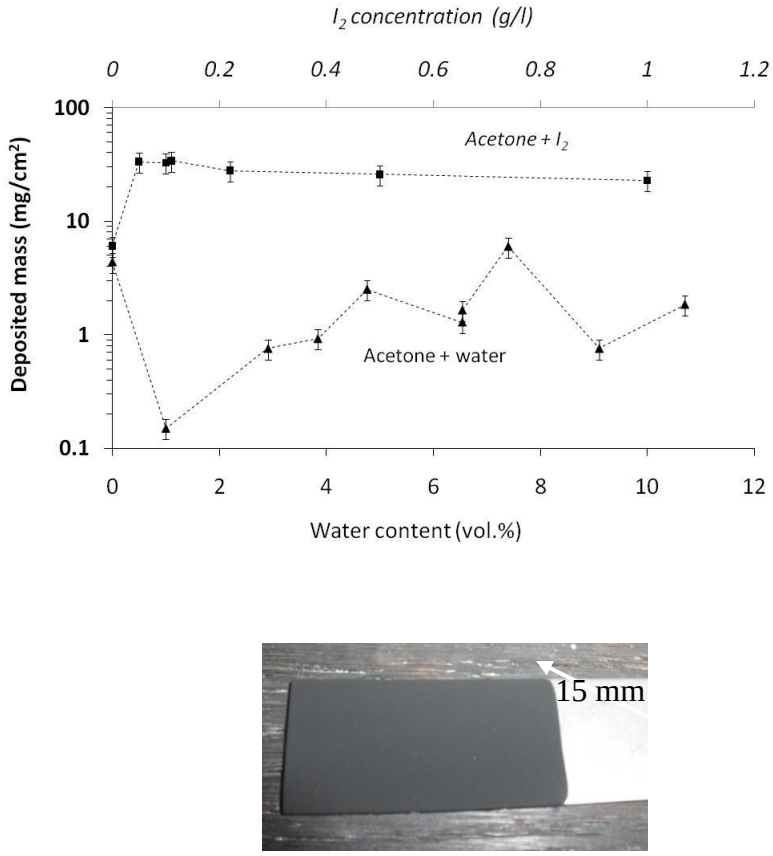

Figure 9. (a) YBCO deposit mass per unit area as a function of the iodine content and water in 10 vol.% acetone suspensions. (b) Picture of a deposit obtained applying 200V for 60 s in a 10 g/l suspension dispersed by the addition of 0.2 g/l of I_2.